Structural Engineering and Mechanics, *Vol. 63, No. 3 (2017) 347-359*
DOI: https://doi.org/10.12989/sem.2017.63.3.347

Numerical analysis of reaction forces in blast resistant gates

Hasan Al-Rifaie* and Wojciech Sumelka[a]

Poznan University of Technology, Institute of Structural Engineering, Piotrowo 5, 60-965 Poznan, Poland

(Received February 23, 2017, Revised April 18, 2017, Accepted April 19, 2017)

Abstract. Blast resistant gates are required to be lightweight and able to mitigate extreme loading effect. This may be achieved through innovative design of a gate and its supporting frame. The first is well covered in literature while the latter is often overlooked. The design of supporting frame depends mainly on the boundary conditions and corresponding reaction forces. The later states the novelty and the aim of this paper, namely, the analysis of reaction forces in supporting structure of rectangular steel gates subjected to “far-field explosions”. Flat steel plate was used as simplified gate structure, since the focus was on reaction forces rather than behaviour of gate itself. The analyses include both static and dynamic cases using analytical and numerical methods to emphasize the difference between both approaches, and provide some practical hints for engineers. The comprehensive study of reaction forces presented here, cover four different boundary conditions and three length to width ratios. Moreover, the effect of explosive charge and stand-off distance on reaction forces was also covered. The analyses presented can be used for a future design of a possible “blast absorbing supporting frame” which will increase the absorbing properties of the gate. This in return, may lead to lighter and more operational blast resistant gates.

Keywords: blast resistant gates; reaction forces; ConWep

1. Introduction

An explosion nearby a building can cause catastrophic damage to buildings’ structural and non-structural elements. Loss of life or injury is a consequence of blast shock, structural collapse, debris impact, fire or smoke (Ngo *et al.* 2007). The key to a successful design of a protective system is the detection of weakest points in the structure. A research at the United States Air Force Research Laboratory (Anderson and Dover 2003), emphasizes that doors or gates have always been one of the weakest points in many structures. The traditional heavy and solid design of gates led to higher manufacturing cost and poor operational performance (Chen and Hao 2014). These massive doors are not suitable for general-purpose usage such as armoured cars, airplanes and residential premises. Accordingly, gates are required to be lightweight and able to mitigate extreme loading effect. This may be achieved through innovative design of a gate and its supporting frame. The first is well covered in literature while the latter is often overlooked (Anderson and Dover 2003). Therefore, this paper tried to fill this scientific gap since the design of supporting frame depends mainly on boundary conditions and corresponding reaction forces.

In terms of the gate itself, several energy absorbing techniques were investigated by researchers. One of the studies of the US Air force Research Laboratory recommends the use of Accordion-Flex Door (Anderson and Dover 2003). The proposed door is an accordion panel that is allowed to deform significantly when exposed to blast pressure. Chen and Hao (2012), introduce a new configuration for blast doors which consists of a double-layered panel with a structural form of multi-arched-surface. Blast resistance and energy absorption capacities were numerically investigated using FE code. The research proved that multi-arch panel can sustain higher blast loads. The use of innovative materials instead of changing structural form was of interest to Yun *et al.* (2014). The study suggests the use of aluminium alloy foam to improve blast pressure mitigation. Significant reduction in permanent deformation was recorded when using high density foam (Yun *et al.* 2014). These techniques focus on absorbing the blast energy by the gate structure and reduce the amount of forces transferred to the supporting frame.

Supporting frames of blast resistant gates play an important role in blast events. In literature, and according to the author survey, the frames of blast resistant gates are usually assumed to be rigid or stiff enough to hold the gate, and that the failure would appear either in the gate itself or in the hinges connecting the gate to the supporting frame. This may be correct when the gate itself is able to absorb the dynamic energy. However, for better performance, the supporting frame may also be designed to absorb the dynamic impact through incorporation of passive damping systems. One of the very few studies that implement a damping system is the one done by Fang *et al.* (2008). The study claims that “*the resistance of the blast doors can be increased obviously by the springs and the dampers, and the shorter the duration of the loads, the more effective the increasing of the resistance*”. The design of supporting frame is linked directly to boundary conditions and

∗Corresponding author, Ph.D. Student
E-mail: hasan.al-rifaie@put.poznan.pl
[a]Professor
E-mail: wojciech.sumelka@put.poznan.pl

http://www.techno-press.com/journals/sem&subpage=7 ISSN: 1225-4568 (Print), 1598-6217 (Online)

corresponding reaction forces.

Boundary conditions and reaction forces are crucial as they play an important role in the failure mechanism of plates. Bonorchis and Nurick (2007) mention that "*few papers have been published on the effect of boundary conditions on the high strain rate response of plates subjected to blast (impulsive) loading*". An experimental study, by Nurick and Shave (1996), address the rupture scenarios in a fully clamped square and circular plates subjected to uniform impulsive load. Three failure modes were highlighted which are mode I (large ductile deformation), mode II (tensile-tearing and deformation) and mode III (transverse shear). The study concludes that the failure mode was directly attributed to the boundary condition. A recent comprehensive review in 2016 by Yuen *et al.* (2016), summarizes experimental studies conducted in the last 25 years in the field of thin plates subjected to air-blast loading. The review paper groups the studies according to four classifications; which are loading type (uniform, localized), Plate geometry (Circular, quadrangular, stiffened, flat), failure modes and boundary conditions. The paper confirms that the severity and location of failure modes, mentioned earlier, is primarily determined by spatial distribution of the blast loading across the plate surface, and the plate boundary conditions. Rudrapatna *et al.* (1999) show the numerical results for clamped, thin square steel plates subjected to blast loading. Their study covers the effect of material and geometrical non-linearities in addition to strain rate sensitivity. The outcomes clearly demonstrate the influence of shear near boundaries on the failure mechanism. In addition to the mentioned role of boundary conditions, reaction forces are affected directly by the loading type (uniform or localized).

Far-field blast pressure apply uniform loading on the face of the target. Borenstein and Benaroya (2013), mention that the use of Hopkinson-Cranz scaled distance Z to find blast load parameters is accurate when the target is relatively far from the source of explosion. Their research deals with the elastic deformation of steel plate due to near field explosion. Results from the analytical and FE models show response sensitivity to plate thickness and stand-off distance (Borenstein and Benaroya 2013). A non-linear SDOF model has been examined by Feldgun *et al.* (2016) to simulate the blast response of elastic thin rectangular plates that undergo large deflections. A comparison of static and dynamic nonlinear solutions is performed. Both simply support and fully clamped boundary conditions were taken into account with the assumption of uniform blast pressure loading (Feldgun *et al.* 2016). The distribution of blast pressure on fully clamped circular steel plates has been studied by Jacob *et al.* (2007). Based on theoretical and experimental analyses, the study confirms that "*at stand-off distances less than the plate radius, the blast load is considered to be focused (localized). For stand-off distances greater than the plate radius, the loading is considered uniformly distributed over the entire plate area*"(Jacob *et al.* 2007). Therefore, loading type (uniform, localized) is changing based on the explosive mass or its centroid stand-off distance.

The effect of changing the explosive mass or its centroid stand-off distance on the response of plates is studied by some researchers, such as (Jacob *et al.* 2007, Borenstein and Benaroya 2013, Curry and Langdon 2016). Curry and Langdon (2016), use high speed imaging and digital image correlation techniques to investigate the transient deformation and strain evolution of a deformable plate for different charge and stand-off distances. The work concludes that permanent deformation dropped with increasing stand-off distance and rose linearly with increasing the explosive mass. The results of another study, by Aune *et al.* (2017), provides blast-structure response spectrum based on numerical and experimental investigations. The spectrum provide the change of permanent mid-point deflection with respect to the steel plate thickness $(x - axis)$ and stand-off distance $(y - axis)$. The study confirms the decrease in the mid-point deflection with respect to the increase in the stand-off distance. The reviewed literature in this field bases their calculations on analytical, numerical or physical models.

Development of simplified and accurate models, for estimating the structural response due to blast waves, is a subject of extensive studies in the last decades (Wang *et al.* 2013). Explosion are sudden and rapid release of energy to its surroundings in the form of moving blast wave (Mannan 2013). It is obvious that properly planned field testing with live explosives reflects the most reliable outcomes. However, legal permissions, consecutive cost and time limits are all obstacles that make this choice harder to select (Mazek 2014). Therefore, mathematical/virtual methods including analytical analysis, numerical simulations or laboratory techniques are most important alternatives at the initial stage of product development. Numerical simulations provide an alternative for more complex structures, where analytical option is time consuming or even impossible to accomplish. Computer programs are used for prediction of blast loading action on the structure, calculation of structural response or both. SIMULIA ABAQUS software has been used in this study. It can be noticed that the use of FE codes has been extensively covered by researchers such as Lee *et al.* (2009), Gong *et al.* (2009), Sielicki (2013), Amadioa and Bedon (2014), Sielicki *et al.* (2017).

To conclude, based on this literature survey, deformation and failure of blast resistant gates were broadly examined, with specific attention to four factors; boundary conditions, aspect ratios, loading type, charge and stand-off distance. In addition, the design of supporting frame depends mainly on the boundary conditions, loading pattern and corresponding reaction forces. The later states the novelty and the aim of this paper, namely, the analysis of reaction forces in the supporting structure of rectangular steel gates subjected to "far-field explosions". Flat steel plate was used as simplified gate structure, since the focus was on reaction forces rather than behaviour of gate itself. The analyses include both static and dynamic cases using analytical and numerical methods to emphasize the difference between both approaches, and provide some practical hints for engineers. The comprehensive study of reaction forces presented here, cover four different boundary conditions and three length to width ratios. Moreover, the effect of explosive charge and stand-off distance on the reaction

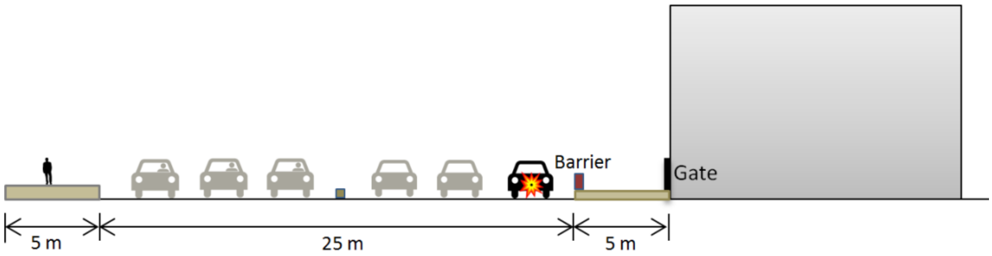

Fig. 1 Blast scene under consideration

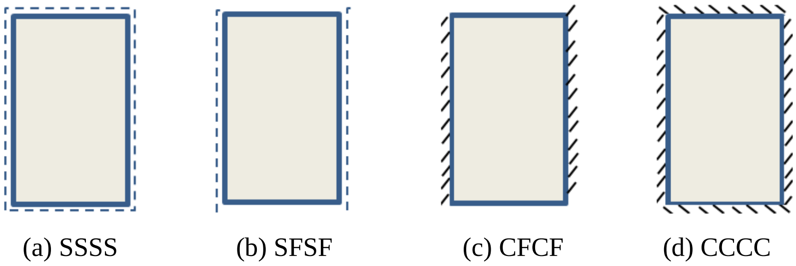

Fig. 2 Selected boundary conditions

forces was also covered. The objectives of this paper are:

- Finding the reaction forces of plates subjected to static uniform pressure (as an equivalent static approximation of a far-field explosion) using numerical simulation (Abaqus/Standard), then validating the results with analytical solution at specific points.
- Finding the reaction forces of plates subjected to dynamic loading (using numerical method (Abaqus/explicit) and comparing the results with the static outcomes. Then, selecting the optimum BC case for possible future implementation of passive damping systems.
- Examining the influence of changing explosive mass or its position on reaction forces.

2. Case study

Size of blast resistant gates ranges from small doors to large gates with unlimited possibilities of length to width ratio (aspect ratio). Therefore, in this study, the discussion would be based on the most common aspect ratios as an alternative, as the focus here was on the distribution and change of reaction forces rather than solution for a specific case. In terms of boundary conditions, four symmetric boundary conditions were selected as they are the most common combinations used in blast resistant gates.

The pressure due to blast incident varies according to the mass of the explosive (M) and its stand-off distance (R). In urban areas, where sensitive infrastructure exists, such as embassies or parliaments, traffic should be limited to passenger vehicles (i.e., no trailers or load-carrying vehicles). Therefore, the mass of the explosive material was assumed to range from 100-1000 kg, which is the possible amount that can be held in motorcycle or normal vehicle. In terms of stand-off distance, barriers should be provided to prevent near field explosion scenarios. In return, protection from direct shock, heat or debris impact can be achieved. The stand-off distances were assumed to be ranging from 5-30m based on the street width. The blast scene is shown in Fig. 1. In the following sub-sections, more details are provided for geometry, boundary conditions, material and loading.

2.1 Geometry

The height to width ratio of a plate, i.e., aspect ratio (AR), can be of any magnitude ranging from 1 (square plate) to ∞. However, deflection and reaction factors do not change significantly when AR$>$ 2, since the plate starts to behave as one way strip. Therefore, three ARs are studied here, which are $1, 1.5$ and 2.

For static analysis, the dimensions of a plate and magnitude of the load were treated as model parameters in a non-dimensional manner. However, for a dynamic problem, the pressure from an explosion does not have single value and changing over time. So, the problem cannot be solved in non-dimensional manner. For that reason, and to allow physical understanding, the following values were assumed for dynamic analysis:

- for AR=1, the plate dimensions are 1000×1000 mm
- for AR=1.5, the plate dimensions are 1000×1500 mm
- for AR=2, the plate dimensions are $1000x2000\ mm$
- Plate thickness= 10 mm

2.2 Boundary conditions

Generally, each edge of the plate can either be free (F), simply supported (S), or Clamped (C) (Lim *et al.* 2007). Therefore, there are 21 possible boundary conditions (Chakraverty 2008). Here, four common symmetric boundary conditions were taken into account in the analysis of the steel plate. Those boundary cases are; four edges

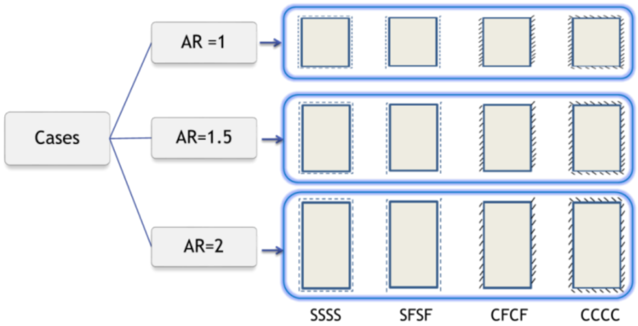

Fig. 3 The 12 cases under consideration (four BCs and three ARs)

simply supported (SSSS), two opposite edges simply supported and two free (SFSF), two opposite edges clamped and two free (CFCF) and the last case is four edges clamped (CCCC), see Fig. 2.

The four BCs and the three ARs lead to 12 cases in total as shown in the tree diagram (Fig. 3).

2.3 Material

An elastic material model would be sufficient for the static analysis part of this study, since no material hardening or damage was expected. However, when changing the mass of the TNT or its position in dynamic simulations (Section 4.3), elastic model may no longer represent the real behaviour. For that reason and for the unity of the analysis, an elasto-plastic model with damage initiation was used for both static and dynamic simulations. The used material is "Weldox 460 E Steel". Weldox is a class of thermo mechanically rolled ferritic structural steels that offers both ductility and high strength (Børvik *et al.* 2001). Plasticity and damage are defined using Johnson-Cook parameters. Børvik *et al.* (2001) give material constants for the Weldox 460 E Steel as shown in Table 1. Such a choice is argued based on previous results by Sumelka and Łodygowski (2011), Łodygowski *et al.* (2012) and Szymczyk *et al.* (2017).

2.4 Loading

Far-field explosion was selected as it generates flat and uniform pressure. Hence, more valid comparison could be made between the dynamic pressure and its static approximation. As there are four factors affecting the results, namely, BCs, ARs, M and R, one factor was modified at a time to see its influence on reaction forces.

First, the value of M and R were fixed to 100 kg and 30 m, respectively. This was to investigate the effect of BCs and ARs on reaction forces and it allowed clearer comparisons between static and dynamic solutions. According to TM-5 1300 (TM5-1300 1990), this combination of mass and stand-off distance generates 0.06 MPa peak reflected over-pressure. This uniform pressure value was used for static analyses (analytical and numerical). For dynamic simulations, ConWep tool was implemented with surface blast incident wave.

Table 1 Material constants for Weldox 460 E Steel (adopted from Børvik *et al.* 2001)

Category	Constant	Description	Unit	Value
Elastic Constants	E	Modulus of Elasticity	MPa	200×10^{3}
	ν	Poisson's ratio	-	0.33
Density	ρ	Mass density	t/mm^3	7.85×10^{-9}
Yield stress and strain hardening	A	Yield Strength	MPa	490
	B	Ultimate Strength	MPa	807
	n	-	-	0.73
Strain-rate hardening	$\dot{p}_0 . \dot{r}_0$	Reference Strain rate	S^{-1}	5×10^{-4}
	C	-	-	0.0114
Damage evolution	D_c	Critical Damage	-	0.3
	p_d	Damage threshold	-	0
Adiabatic heating and temperature softening	C_p	Specific heat	mm^2.K/S^2	452×10^{6}
	χ	Taylor Quinney empirical constant/inelastic heat fraction	-	0.9
	α	Coefficient of thermal expansion	K^{-1}	1.1×10^{-5}
	T_m	Melting Temperature	K	1800
	T_0	Room Temperature	K	293
	m	-	-	0.94
	K	-	-	0.74
Fracture Strain Constants	D_1	-	-	0.0705
	D_2	-	-	1.732
	D_3	-	-	-0.54
	D_4	-	-	-0.015
	D_5	-	-	0

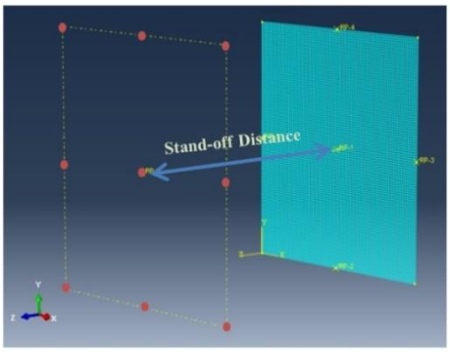

Fig. 4 Variation of the explosive centroid position in x, y and z directions

Second, the mass of the explosive material and its position was modified in section 4.3 to examine the effect of such a variation on the reaction forces. The value of M was increased gradually with keeping R fixed at 30 m. Five steps were taken at 200 kg, 400 kg, 600 kg, 800 kg and 1000 kg. The position of the centroid of the explosive material depends on the stand-off distance (z-direction) and the position in a plane parallel to the plate under consideration, x and y directions (Fig. 4). The stand-off distance (R) was increased from 5-30 m (5 m step) to see

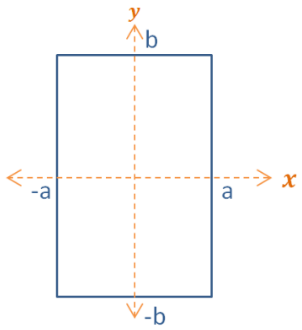

Fig. 5 Plate configuration

its effect on the reaction forces (with keeping the mass at 100 kg and its centroid coincident with the center of the plate). Then, the position of the centroid was modified to 9 different positions on a plane parallel to the plate under consideration (with keeping the mass at 100 kg and its centroid at $R = 30$ m), as shown in Fig. 4. Results for the effects of variation in explosive mass and position are shown in section 4.3.

3. Methodology

The analyses implemented in this paper include both static and dynamic cases using analytical and numerical methods. Here is a brief description of the methodology.

3.1 Static analysis

Classical plate theories provide analytical solutions for reaction forces along the edges of thin elastic plates. The boundary conditions, dimensions and loading scenario are the key elements in the solution. Early papers in this field; such as Love (2013), Timoshenko and Woinowsky-Krieger (1959) and Meleshko (1997); mention that fully simply supported plate (SSSS) was first solved by Navier (1823) through implementing a double trigonometric series. Then, plate with two opposite edges simply supported and the other two free (SFSF) was solved by Levy (1899). After that, clamped plate conditions were considered by Koialovich (1902), Hencky (1913) and Boobnoff (1914). The solutions of the previous mentioned scientists are well quoted in books of plate theory, theory of elasticity or research articles. A brief description is discussed here.

Consider a homogeneous isotropic elastic thin plate, of sides $a' = 2a$, $b' = 2b$. The plate is subjected to a uniformly distributed load of q, with the center of the plate lying on the origin of the cartesian coordinates Oxy. The plate occupies the region $-a \leq x < a$ and $-b \leq y < b$ (Fig. 5).

Then, the plate governing equation is

$$\Delta^2 w = \frac{q}{D} \ , \tag{1}$$

where,

Δ is a two-dimensional laplace operator

$$\Delta \equiv \frac{\partial^2}{\partial x^2} + \frac{\partial^2}{\partial y^2}, \tag{2}$$

D is the bending stiffness

$$D \equiv \frac{h^3 E}{12\,(1-\upsilon^2)}, \tag{3}$$

E is the modulus of elasticity, h is the plate thickness, υ is the Poisson's ratio and w is the transverse deflection of the middle plane of the plate. Eq. (1) can be solved through satisfying the boundary conditions at the edges. The deflection w is

$$\begin{aligned} w = w_0 + \frac{q}{D}\sum_{n=0}^{\infty}(-1)^n \Big(A_n \frac{\cosh \alpha_n y}{\cosh \alpha_n b} + \\ B_n \frac{y}{b}\frac{\sinh \alpha_n y}{\cosh \alpha_n b}\Big) \cos\, \alpha_n x + \\ \frac{q}{D}\sum_{n=0}^{\infty}(-1)^n \Big(C_n \frac{\cosh \beta_n x}{\cosh \beta_n a} + \\ D_n \frac{x}{a}\frac{\sinh \beta_n x}{\cosh \beta_n a}\Big) \cos\, \beta_n y \ , \end{aligned} \tag{4}$$

where w_0 is a particular solution satisfying $\Delta^2 w_0 = \frac{q}{D}$ and where

$$\alpha_n \equiv \frac{(2n+1)\pi}{2a} \qquad \beta_n \equiv \frac{(2n+1)\pi}{2b}. \qquad (n = 0,1,2,\dots) \tag{5}$$

The particular solution w_0 is taken in the form of a symmetrical polynomial of the fourth order in x and

$$\begin{aligned} w_0 = c_0 + c_1 x^2 + c_2 y^2 + c_3 x^4 \\ + c_4 x^2 y^2 + c_5 y^4. \end{aligned} \tag{6}$$

This solution should satisfy the plate equation so that

$$3c_3 + c_4 + 3c_5 = \frac{q}{8D} \ . \tag{7}$$

Once w is known, bending moments M_x, M_y and twisting moment M_{xy} can be calculated as follow

$$\begin{aligned} M_x &= -D\left(\frac{\partial^2 w}{\partial x^2} + \nu\frac{\partial^2 w}{\partial y^2}\right) \ , \\ M_y &= -D\left(\frac{\partial^2 w}{\partial y^2} + \nu\frac{\partial^2 w}{\partial x^2}\right) \ , \\ M_{xy} &= -(1-\nu)D\frac{\partial^2 w}{\partial x \partial y} \ . \end{aligned} \tag{8}$$

Shear forces Q_x, Q_y and effective shear forces V_x, V_y can be found from

$$Q_x = -D\frac{\partial \Delta w}{\partial x} \ , \ Q_y = -D\frac{\partial \Delta w}{\partial y} \ , \tag{9}$$

$$\begin{aligned} V_x &= -D\left[\frac{\partial^3 w}{\partial x^3} + (2-\nu)\frac{\partial^3 w}{\partial x \partial y^2}\right] \ , \\ V_y &= -D\left[\frac{\partial^3 w}{\partial y^3} + (2-\nu)\frac{\partial^3 w}{\partial x^2 \partial y}\right] \ . \end{aligned} \tag{10}$$

The detailed derivation of the deflection, moment and shear coefficients, α , β *and* γ, respectively, are available in (Timoshenko and Woinowsky-Krieger 1959) for different boundary conditions and are out of the scope of this study. The magnitudes of β *and* γ are given in Table 2 (under analytical columns) for each of the four cases under consideration; SSSS, SFSF, CFCF and CCCC. Therefore, If the dimensions of the plate (L,W and t) are given, and based on the moment and shear factors, β *and* γ, one can find

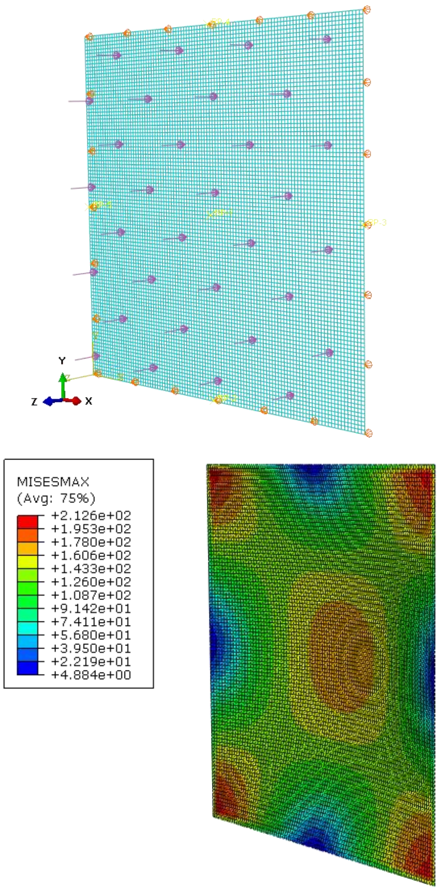

Fig. 6 Loading of the SSSS case, AR=1, and the corresponding Mises stresses

the moment and shear at the centre of supporting edges using

$$M_y = \beta q a'^2, \qquad Q = \gamma q a' \tag{11}$$

The achieved moment and shear represent the reaction forces at the centre of supporting edges. These values solved at certain points were used for validation of the reaction forces along the plate edges acquired from Static numerical analysis.

The same 12 cases (in Fig. 3), were solved numerically using Abaqus/Standard. This was to get the reaction forces at every point on the supporting edges. The achieved results were then compared with the analytical solution solved for specific points. The modelling in Abaqus/CAE had the following properties:

- Deformable shell of planar type
- FE type = S4 (a 4 node doubly curved general purpose shell element)
- Homogenous continuous plate section of thickness t=10 mm
- Mesh size=10 mm
- Linear analysis

Although the aim of the research was the analyses of reaction forces rather than the plate behaviour, it was crucial to check the plate situation under blast loading (i.e., elastic, plastic or in the damage range). Therefore, Mises stresses were checked for all cases. It was found that the Maximum Mises stress (across the thickness of the plate) over the whole plate in all cases was under the yield point of the steel material used (i.e., in elastic range). Fig. 6 shows the loading pattern of the SSSS case with AR=1 and the corresponding Max. Mises stress (in MPa).

3.2 Dynamic analysis

Blast simulation (as a dynamic load) can be performed in Abaqus using either ConWep or CEL tools. ConWep (Conventional Weapons) was developed by the US army and then was incorporated in the Abaqus solver (Hyde 1991). It is a blast loading predictive tool that is based on real-field experimental data from Kingery and Bulmash (1984) for different TNT mass and stand-off distance combinations. The benefit of using this tool is that the blast loading is applied directly on the target without the need to model the surrounding atmosphere. This makes the computations less expensive. However, in that case, blast pressure estimation would not be linked to scene configuration such as reflection (of multiple blast waves), shadowing (object is blocking a surface of the structure from direct blast wave) or confinement (due to geometry of the structure). In ConWep model, there are two types of waves, spherical waves for explosions in mid-air and hemispherical waves for explosions at ground level in which ground effects are included (Dassault Systèmes 2013).

The second tool is CEL that employs Coupled Eulerian-Lagrangian blast load analysis by modelling the structure and the surrounding ambient medium. This technique deals with the blast wave propagation in the air, the blast wave interaction with the structure and the related structural behaviour (Mougeotte *et al.* 2010). CEL tool automate the whole process with less user inclusion in defining "angles of incidents" or reflection surfaces. In addition, CEL model computations are more expensive and time-consuming (Mougeotte *et al.* 2010). It is totally the analyst decision whether to choose ConWep or CEL based on the complexity of the blast scene and the number of possible blast scenarios that should be analysed.

In section 3.1, the 12 cases were analysed for static uniform pressure as far-field explosion. Here, in this section, the response of steel plates (12 cases) is examined under ConWep loading using Abaqus/Explicit numerical solver. The finite element type used is an explicit, linear, quadrilateral four-node, doubly-curved general purpose shell $S4$ element (size=10×10 mm). The blast incident was set at time $t_{incident}$= 0, and the shock wave travelled 30 m and first hit the plate at arrival time t_a=56 ms. In addition, the pressure evolved from the blast was checked using IWConWep option. The amount and distribution of the pressure are shown in Fig. 7. The peak value is 0.062 MPa which is quite similar to the estimated value of 0.06 MPa in TM-5 US code (TM5-1300 1990). Results of these numerical simulations, for the 12 cases under consideration, subjected to this dynamic loading which is equivalent to the static pressure, are all presented in section 4.2. Then, the effects of variation in explosive mass or position on reaction forces are presented in section 4.3 based on loading conditions discussed earlier in section 2.4.

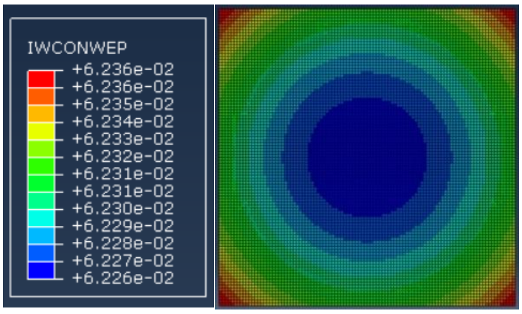

Fig. 7 The amount and distribution of pressure (in MPa) generated from ConWep ($M = 100Kg$ TNT, $R = 30m$) on the surface of steel plate, AR=1

Table 2 Shear and moment factors at horizontal and vertical edge mid-points for both analytical and numerical solutions (under static loading)

BC	b/a	At centre of Vertical Edges				At centre of Horizontal Edges			
		Moment factor β		Shear factor γ		Moment factor β		Shear factor γ	
		Analyt.	Num.	Analyt.	Num.	Analyt.	Num.	Analyt.	Num.
SSSS	1	0	0	0.4200	0.4200	0	0	0.4200	0.4200
	1.5	0	0	0.4850	0.4800	0	0	0.4850	0.4800
	2	0	0	0.5030	0.4950	0	0	0.5030	0.4950
SFSF	1	0	0	0.4687	0.4445	0	0	0	0
	1.5	0	0	0.4860	0.4780	0	0	0	0
	2	0	0	0.4940	0.4920	0	0	0	0
CFCF	1	0.0816	0.0815	0.4880	0.4840	0	0	0	0
	1.5	0.0824	0.0823	0.4953	0.4952	0	0	0	0
	2	0.0830	0.0830	0.4992	0.4992	0	0	0	0
CCCC	1	0.0513	0.0513	0.4413	0.4390	0.0513	0.0513	0.4413	0.4390
	1.5	0.0756	0.0756	0.5140	0.5130	0.0570	0.0569	0.4654	0.4625
	2	0.0829	0.0829	0.5160	0.5160	0.0570	0.0569	0.4639	0.4610

The selection of the mesh size (10 mm) was based on a parametric study of the element size to examine the accuracy of the computed results. Reducing the element size smaller than 10mm showed no significant change in the reaction forces and led to longer computation time (cf. Sielicki and Stachowski 2015). Therefore, the 10 mm element size found to be adequate. The ‘automatic’ option for time step size was selected in Abaqus/Explicit solver, to allow quick and accurate convergence of the analysis.

4. Results and discussion

4.1 Static analysis

When the solution is based on static loading, with one uniform pressure and bending stiffness, the reaction forces and moments can be converted to shear and moment factors using Eq. (11). This would allow comparison with the analytical factors to check the numerical simulation against analytical solution at specific points. As mentioned earlier, in this study, the analytical solution was conducted for two specific points which were the mid-points of both horizontal and vertical supporting edges. Table 2 shows the shear and

Table 3 Analytical and numerical solutions for reaction factors at vertical edge midpoint under static loading

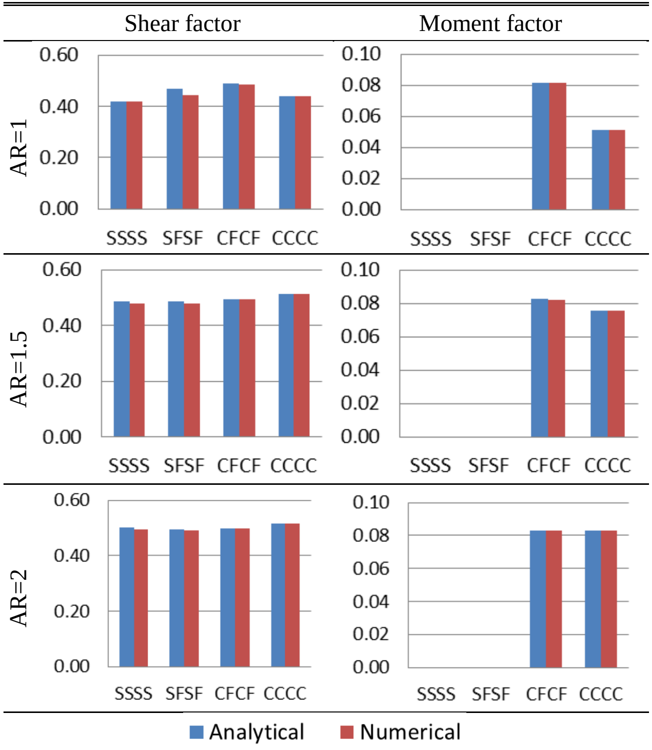

moment factors at horizontal edge and vertical edge mid-points. The table provide both analytical and numerical solutions (under static loading).

Table 3 was generated based on Table 2 for validation and remarks. It shows 6 bar charts of 3 rows and 2 columns. The rows correspond to the three ARs while the columns are for the shear and moment factors, respectively. Based on the bar charts in Table 3, the following points can be concluded:

- The analytical results were of high similarity to the numerical outcomes.
- Results were compatible with factors achieved by other researchers, (Timoshenko and Woinowsky-Krieger 1959) and (Lim *et al.* 2008).
- The shear and moment factors for the SFSF and CFCF were less affected by ARs as the other edges were already not supported.
- The moment factor of CCCC case had increased significantly with the increase of AR.
- The SSSS case had slight increase in shear factors due to AR change.

Detailed reaction forces due to static loading (Abaqus/Standard), at every point along the vertical and horizontal edges, are presented in the first columns of Table 5, Table 6 and Table 7, for AR=1, 1.5 and 2, respectively. This is to provide easier comparison with dynamic analyses.

4.2 Dynamic analysis

The distribution pattern and the magnitude of the reaction forces are usually changing at each time increment in dynamic loading. As an example, Fig. 8 shows the

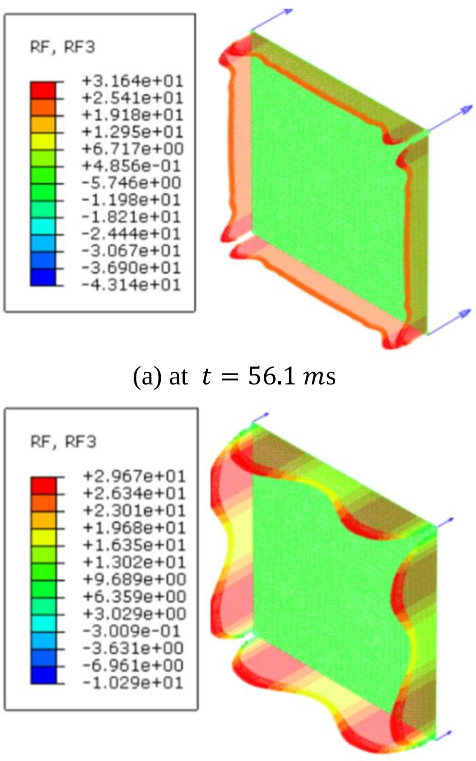

(a) at $t = 56.1\ ms$

(b) at $t = 69.5\ ms$

Fig. 8 Distribution of reaction forces (in N/mm) along the edges at two different time steps, SSSS case, AR=1

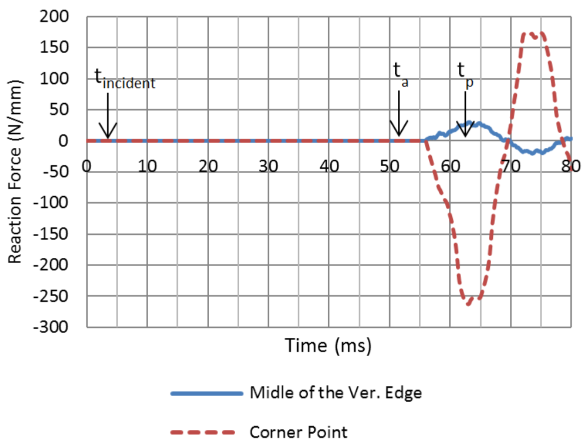

Fig. 9 Reaction force-time history at the vertical edge mid-point and a corner point, (SSSS, AR=1) case

distribution of reaction forces along the edges of SSSS square plate at two different time steps, 56.1 and 69.5 ms.

However, it is important to mention that there is single time step that provides peak reactions at all edge points (t_p). This time step is usually few milliseconds after the arrival of the shock wave (t_a). Fig. 9 below shows reaction force-time history at vertical edge mid-point and a corner point for (SSSS, AR=1) case. It clarifies how the shock wave travelled 30 m and first hit the plate at t_a=56 ms. Then, the reaction forces start to increase until reaching peak values at t_p=62 ms.

It was found that t_p was different from a case to another based on boundary conditions. Table 4 lists $t_{incident}$, t_a, t_p and the time required to reach peak reaction forces for every BCs (ordered from the shortest to the longest).

Table 4 Time required to reach peak reaction forces for all BCs (ordered from the shortest to the longest)

BC	$t_{incident}$	t_a	t_p	time to peak response (t_p - t_a), in ms
CCCC	0	56	61	5
SSSS	0	56	62	6
CFCF	0	56	64	8
SFSF	0	56	73	17

Maximum Mises stresses (in all cases) were checked for this dynamic loading and showed to be less than the yield stress of the steel material used. In other words, the cases were within the elastic range.

For this dynamic loading (which is equivalent to the static pressure discussed in section 2.4), the reaction forces along the edges of the plates are shown in the second columns of Table 5, Table 6 and Table 7, for AR= 1, 1.5 and 2 respectively. The tables sunmmurize static (Abaqus/Standard) and dynamic (Abaqus/Explicit) simulations for all 12 cases under investigation. In these tables, it is important to highlight that the moment and shear distribution curves for the horizontal edges were drawn for only SSSS and CCCC cases as other cases (SFSF and CFCF) have free horizontal edges.

Based on the results shown in Tables 5 to 7, the following points can be underlined:

- Each BC (SSSS, SFSF, CFCF, CCCC), has a specific *‘distribution pattern’* of reaction which stayed the same regardless to loading condition (static, dynamic), AR (1, 1.5, 2) or edge (horizontal, vertical). However, the magnitudes or values of these reaction forces were changing.
- Simply-supported cases, SSSS and SFSF, show a flat curve of almost uniformly distributed reaction forces along supporting edges, with high concentrated nodal forces at the corners.
- CFCF case has usually uniformly-distributed force and moment along vertical edge. Then, slight rise can be noticed before the corners followed by sharp negative drop at the corners.

Reaction forces and moments from CCCC case revealed the opposite by having least values at the corners and maximum values at the edges mid points.

The distributed reaction forces on the edges of the plates due to dynamic loading had different values than the static one. The justification is related to the inertia forces that changes the response depending on the boundary conditions BC and aspect ratios AR. To compare the values given in Tables 5 to 7, the dynamic/static ratio (D/S) was calculated for each point along the edges. Then the mean value was governed. This value represents the average increase or decrease in the reaction for a single edge of a case. Fig. 10 shows the average dynamic/static ratio $(D/S)_{avg.}$ for all cases under investigation. Values over one mean that reaction forces due to dynamic loading are higher than the corresponding static reaction forces. Values less than one,

Table 5 Comparison between reaction forces along the edges of steel plates, with **AR=1** and different BCs, using dynamic (Abaqus/Explicit) and the Static (Abaqus/Standard) analyses, under surface blast as a dynamic loading (TNT, $M = 100$ kg, $R = 30$ m) and its equivalent static uniform pressure (0.06 MPa)

		Static (Abaqus/Standard)	Dynamic (Abaqus/Explicit)
Reaction Force	Hor. Edge	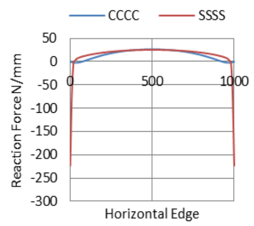	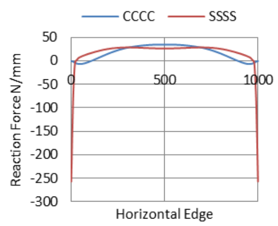
	Ver. Edge	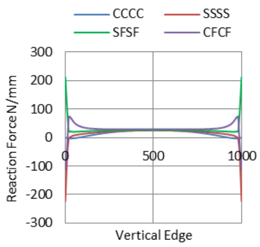	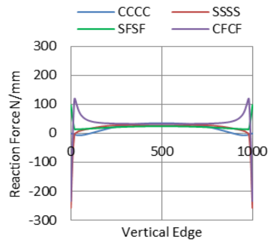
Reaction Moment	Hor. Edge	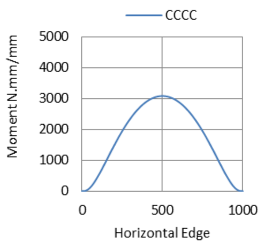	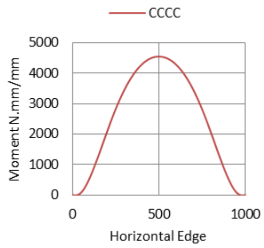
	Ver. Edge	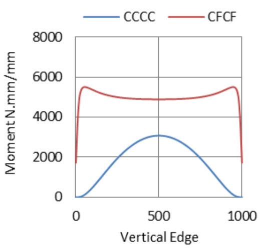	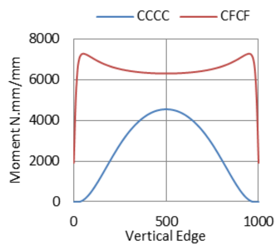

Table 6 Comparison between reaction forces along the edges of steel plates, with AR=1.5 and different BCs, using dynamic (Abaqus/Explicit) and the Static (Abaqus/Standard) analyses, under surface blast as a dynamic loading (TNT, $M = 100$ kg, $R = 30$ m) and its equivalent static uniform pressure (0.06 MPa)

		Static (Abaqus/Standard)	Dynamic (Abaqus/Explicit)
Reaction Force	Hor. Edge	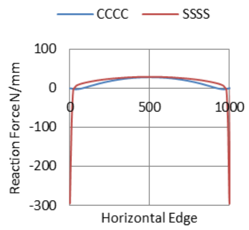	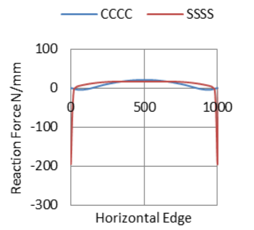
	Ver. Edge	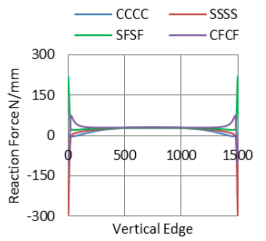	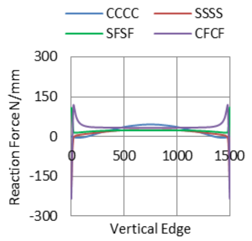
Reaction Moment	Hor. Edge	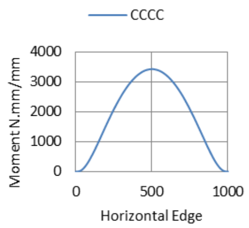	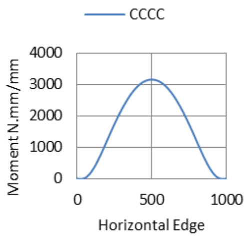
	Ver. Edge	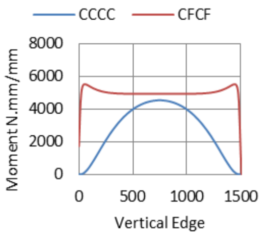	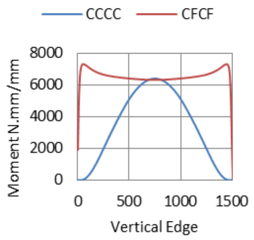

represent the opposite. Based on the results in Fig. 10, the following points can be highlighted:

- For CFCF and SFSF cases, changing AR has no effect on values of $(D/S)_{avg.}$ as the horizontal edges are already not supported. For SSSS and CCCC cases, changing AR has slight effect.
- The highest value is around 2 for CCCC case and drops as low as 0.8 for the SFSF. It is evident here that the more constrains the BCs have, the more shear and moment would be compared to static simulations. The reason to that behavior may be linked to direct transfer of the inertia energy to the supports causing higher shear and moment values. Oppositely, the SFSF case, showed 20% less dynamic response compared to the static. These results are matching the order of BC cases listed in Table 3, where the CCCC was at the top and the SFSF at the bottom of the hierarchy.

Based on the conclusions made earlier, it is totally the designer decision to what BC should be selected for the design of a blast resistant gate. Less constrained BC cases, such as SSSS and SFSF, revealed lower $(D/S)_{avg.}$ than more constrained cases, CCCC and CFCF. In other words, simply supported cases showed better blast mitigation effects since the motion of the plates are greater than that of the clamped cases. These findings can be related to previous research on fluid-structure interaction effects on blast-loaded plates. Kambouchev *et al.* (2006) state that "*the motion of the structure relieves the pressure acting on it, thus reducing the transmitted impulse and, as a consequence, the effects of the blast*". In contrast, for fixed boundary plates, the blast impulse transferred to the plate is maximum (Taylor 1963).

Another important point to mention is that the low "mass per unit area" of the plates analysed in this study also decreases the transmitted impulse to the plate. Lighter

Table 7 Comparison between reaction forces along the edges of steel plates, with AR=2 and different BCs, using dynamic (Abaqus/Explicit) and the Static (Abaqus/Standard) analyses, under surface blast as a dynamic loading (TNT, $M = 100$ kg, $R = 30$ m) and its equivalent static uniform pressure (0.06 MPa)

		Static (Abaqus/Standard)	Dynamic (Abaqus/Explicit)
Reaction Force	Hor. Edge	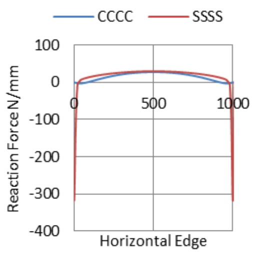	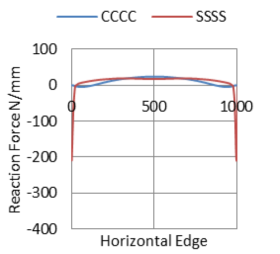
	Ver. Edge	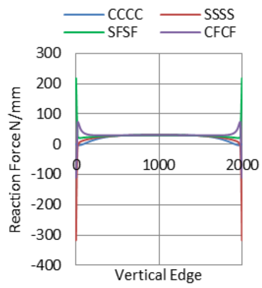	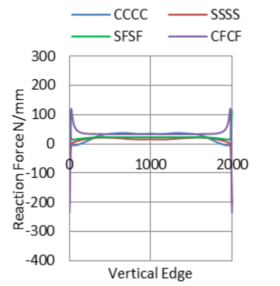
Reaction Moment	Hor. Edge	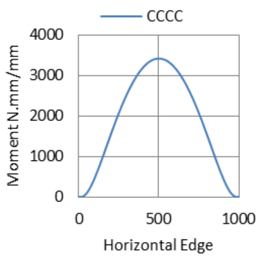	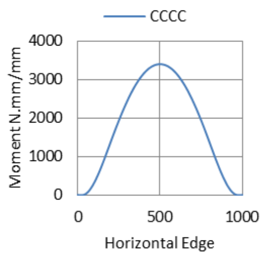
	Ver. Edge	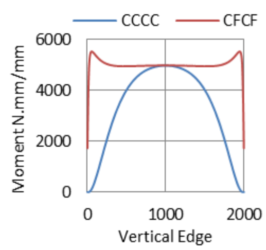	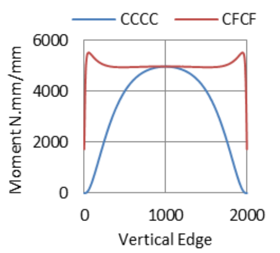

plates acquire velocity quickly thus relieving the pressure acting on the plate (Taylor 1963, Kambouchev *et al.* 2006, Kambouchev *et al.* 2007, Vaziri and Hutchinson 2007).

In short, SFSF or SSSS cases are more favoured upon CCCC and CFCF cases due to their potential blast mitigation. Moreover, the distribution of reaction forces allows efficient implementation of shock absorbers at the supports (especially at the corners where most of reaction appear as nodal forces). A closer look at SSSS and SFSF reaction forces is provided in Fig. 11 for further discussion.

Among the simply supported cases, this study suggests the SFSF case as the optimum option for possible future implementation of passive damping systems in blast resistant gates. This selection was based on the following reasons:

- SFSF case has corner nodal forces less in value than those for the SSSS case. In addition, the time to peak response is $0.017s$ higher than that for the SSSS case, $0.006s$ (Table 4). This combined together lead to lower force rate (change of force per time) and hence lower shock or impact on SFSF supporting frame.
- The reaction force is in the positive range along the length of the vertical edge, i.e. all reactions in one direction opposite to the direction of blast pressure. This is in contrast to the SSSS case where corner nodal forces are in the negative range. This in return leads to easier future application of passive damping systems as they will all behave in the same direction.

4.3 Effects of variation in explosive mass and position

While this study suggests SFSF case as the optimum boundary condition, mass of the explosive material and its position were modified to further examine the effect of such a variation on the reaction forces of SFSF. As mentioned in section 2.4, the value of M was increased gradually with keeping R fixed at 30m. Five steps were taken at 200 kg, 400 kg, 600 kg, 800 kg and 1000 kg. Results revealed that the percentage of increase in reaction forces was linear to some extend when increasing the TNT mass (M), as shown in Fig. 12. Doubling the value of M led to 50% increase in reaction forces, moreover, 97 % change was observed with 4 times rise in the initial mass (200 to

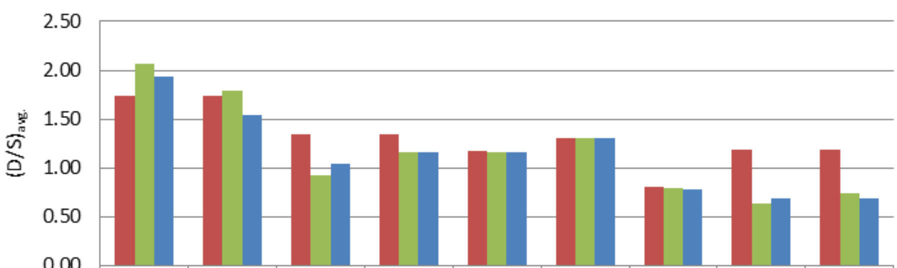

	CCCC RF Hor.Edge	CCCC RF Ver.Edge	CCCC RM Hor.Edge	CCCC RM Ver.Edge	CFCF RF Ver.Edge	CFCF RM Ver.Edge	SFSF RF Ver.Edge	SSSS RF Hor.Edge	SSSS RF Ver.Edge
b/a=1	1.74	1.74	1.34	1.34	1.18	1.30	0.81	1.19	1.19
b/a=1.5	2.06	1.79	0.93	1.16	1.16	1.30	0.79	0.63	0.74
b/a=2	1.94	1.54	1.05	1.16	1.16	1.30	0.78	0.69	0.69

Fig. 10 Values of $(D/S)_{avg.}$ for the horizontal and vertical edges of all cases

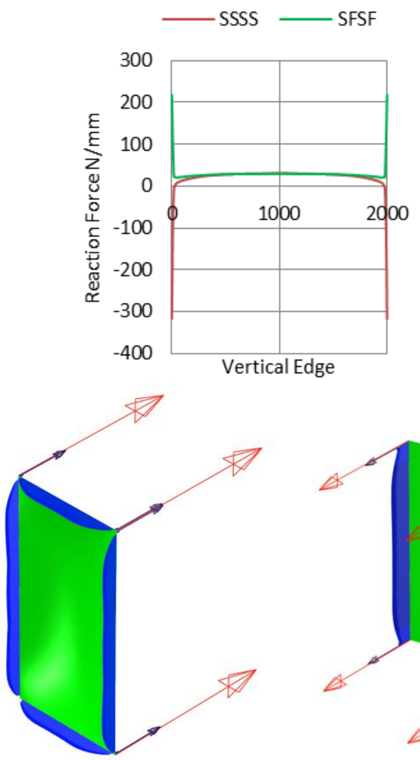

Fig. 11 Comparison between the distribution pattern of reaction forces in SSSS and SFSF cases

800 kg). These outcomes are consistent with the study of Curry and Langdon (2016), which concludes that permanent deformation also raised 'linearly' with increasing the explosive mass.

Results of increasing stand-off distance (R), from 5 m to 30m, with keeping the TNT mass at 100 kg, are shown in Fig. 13. Sharp drop of 81% in the reaction force can be observed with the increase in the stand-off distance from 5 to 15 m. Then, more flat curve can be noticed. It might be also important to mention that the behaviour of the steel plate was within the plastic range, with no damage initiation, throughout the TNT mass range (200 to 1000 kg) and the stand-off distance (5 to 25 m). Elastic behaviour was at $M = 100$ kg and $R = 30$ m, as mentioned in section 4.2.

When changing the position of the centroid of the explosive material in a plane parallel to the plate under consideration, it was found that this sort of change has negligible effect on reaction forces. This is due to the uniform pressure achieved from far-field explosions as confirmed by Feldgun *et al.* (2016). These results were compatible with the conclusions of Jacob *et al.* (2007). In addition, Yuen *et al.* (2016) states that "*when the stand-off distance exceeds the largest plate dimension, loading could be considered to be uniform*".

It is crucial to re-highlight that all the combinations of TNT mass and stand-off distances considered in this study led to far-field uniform loading pattern. Table 8 summarize the studied combinations and their scaled distances Z (with minimum value of 1.1 $\mathrm{m/kg^{1/3}}$). In fact, the validity of using empirical (or ConWep) method becomes

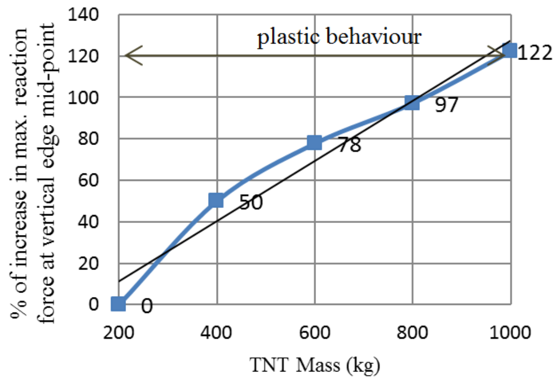

Fig. 12 Percentage of increase in max. reaction force at vertical edge mid-point of the SFSF, AR=1 steel plate, due to the change in TNT mass, at fixed $R = 30$ m

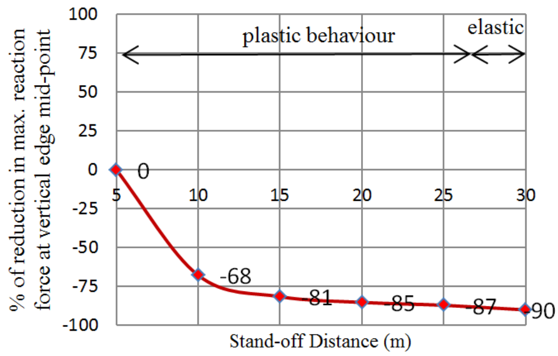

Fig. 13 Percentage of reduction in max. reaction force at vertical edge mid-point of the SFSF, AR=1 steel plate, due to the change in stand-off distance, for TNT mass $M = 100$ kg

Table 8 TNT mass and stand-off distance combinations considered in this study and their scaled distances

		M (mass of TNT in kg)	R (stand-off distances in m)	Z (Scaled distance), $Z = M/\sqrt[3]{R}$
Section 4.2		100	30	6.5
Section 4.3	Changing M	200	30	5.1
		400	30	4.1
		600	30	3.6
		800	30	3.2
		1000	30	3.0
	Changing R	100	25	5.4
		100	20	4.3
		100	15	3.2
		100	10	2.2
		100	5	1.1

questionable when predicting the loading of close-range detonations at scaled distances less than approximately 0.4 $\mathrm{m/kg^{1/3}}$, as the target may be located inside the fireball resulting in an interaction between the expanding detonation products (i.e., the fireball) and the blast overpressure (Rigby *et al.* 2015, Shin *et al.* 2015).

5. Conclusions

In this paper, reaction forces and their influence by boundary conditions, aspect ratios, explosive charge and stand-off distance, were investigated. The analyses cover 12 cases of four different boundary conditions and three aspect ratios. The following conclusions summarize the results:

• Static analyses revealed that the numerical results were of high similarity to the analytical outcomes. In addition, shear and moment factors for the SFSF and CFCF cases were less affected by the aspect ratio (AR) as the other edges are already not supported. The moment factor of CCCC case has increased significantly with the increase of AR ratio unlike the SSSS case which had slight increase in shear factors due to AR change.

• For dynamic loading, distributed reaction forces on the edges of the plates had different values than the static one. The average increase or decrease in the reaction for each supporting edge of a case was examined. For CFCF and SFSF cases, changing AR had no effect on values of dynamic/static ratio $(D/S)_{avg.}$ as the horizontal edges are already not supported. For SSSS and CCCC cases, changing AR had slight influence. The second point is that less constrained BC cases, such as SSSS and SFSF, revealed lower $(D/S)_{avg.}$ than more constrained cases, CCCC and CFCF. In other words, simply supported cases showed better blast mitigation effects since the motion of the plates are greater than that of the clamped cases, thus reducing the transmitted impulse and, as a consequence, the effects of the blast. Therefore, SFSF or SSSS cases are more favoured upon CCCC and CFCF cases due to their potential blast mitigation. Moreover, the distribution of reaction forces in simply supported cases allows efficient implementation of shock absorbers at the supports. This study selects SFSF case as the optimum option for possible future implementation of passive damping systems in blast resistant gates.

• The effect of changing the explosive mass or position on reaction forces was then examined. Five explosive mass steps were taken, $200\ \mathrm{kg}$ to $1000\ \mathrm{kg}$. Results revealed that the percentage of increase in reaction forces due to mass change was approximately linear. On the other hand, the increase in stand-off distance from $5\ \mathrm{m}$ to $15\ \mathrm{m}$ led to a sharp drop of up to 80% in the reaction forces. Then, more flat curve was observed. Changing the position of the centroid of the explosive material in a plane parallel to the plate under consideration had negligible effect on reaction forces. This was true for far-field explosion scenarios, when the stand-off distance was more than the longest plate side. The results were compared with literature and showed high similarity.

The analyses of reaction forces presented in this paper can be used for a future design of a possible '*blast absorbing supporting frame*' which will increase the absorbing properties of the gate. This in return, may lead to lighter and more operational blast resistant gates.

References

Amadioa, C. and Bedon, C. (2014), "FE assessment of dissipative devices for the blast mitigation of glazing façades supported by prestressed cables", *Struct. Eng. Mech.*, **51**(1), 141-162.

Anderson, M. and Dover, D. (2003). "Lightweight, blast-resistant doors for retrofit protection against the terrorist threat", *2nd International Conference on Innovation in Architecture, Engineering and Construction (AEC)*, Loughborough University, UK.

Aune, V., Valsamos, G., Casadei, F., Larcher, M., Langseth, M. and Børvik, T. (2017), "Numerical study on the structural response of blast-loaded thin aluminium and steel plates", *Int. J. Impact Eng.*, **99**, 131-144.

Bonorchis, D. and Nurick, G. (2007), "The effect of welded boundaries on the response of rectangular hot-rolled mild steel plates subjected to localised blast loading", *Int. J. Impact Eng.*, **34**(11), 1729-1738.

Borenstein, E. and Benaroya, H. (2013), "Loading and structural response models of circular plates subjected to near field explosions", *J. Sound Vib.*, **332**(7), 1725-1753.

Børvik, T., Hopperstad, O., Berstad, T. and Langseth, M. (2001), "A computational model of viscoplasticity and ductile damage for impact and penetration", *Eur. J. Mech. A/Solid.*, **20**(5), 685-712.

Chakraverty, S. (2008), *Vibration of plates*, CRC press, USA.

Chen, W. and Hao, H. (2012), "Numerical study of a new multi-arch double-layered blast-resistance door panel", *Int. J. Impact Eng.*, **43**, 16-28.

Chen, W. and Hao, H. (2014), "Experimental investigations and numerical simulations of multi-arch double-layered panels under uniform impulsive loadings", *Int. J. Impact Eng.*, **63**, 140-157.

Curry, R. and Langdon, G. (2016), "Transient response of steel plates subjected to close proximity explosive detonations in air", *Int. J. Impact Eng.*, **102**, 102-116.

Dassault Systèmes (2013), ABAQUS documentation collection.

Fang, Q., Chen, L. and Du, M. (2008), "Theoretical and numerical investigations in effects of end-supported springs and dampers on increasing resistance of blast doors", *Eng. Mech.*, **3**, 035.

Feldgun, V., Yankelevsky, D. and Karinski, Y. (2016), "A nonlinear SDOF model for blast response simulation of elastic thin rectangular plates", *Int. J. Impact Eng.*, **88**, 172-188.

Gong, S., Lu, Y., Tu, Z. and Jin, W. (2009), "Validation study on numerical simulation of RC response to close-in blast with a fully coupled model", *Struct. Eng. Mech.*, **32**(2), 283-300.

Hyde, D. (1991), "Conventional weapons program (ConWep) US army waterways experimental station", Vicksburg, MS, USA.

Jacob, N., Nurick, G. and Langdon, G. (2007), "The effect of stand-off distance on the failure of fully clamped circular mild steel plates subjected to blast loads", *Eng. Struct.*, **29**(10), 2723-2736.

Kambouchev, N., Noels, L. and Radovitzky, R. (2006), "Nonlinear compressibility effects in fluid-structure interaction and their implications on the air-blast loading of structures", *J. Appl. Phys.*, **100**(6), 063519.

Kambouchev, N., Radovitzky, R. and Noels, L. (2007), "Fluid–structure interaction effects in the dynamic response of free-standing plates to uniform shock loading", *J. Appl. Mech.*, **74**(5), 1042-1045.

Kingery, C. and Bulmash, G. (1984), "Technical report ARBRL-TR-02555: air blast parameters from TNT spherical air burst and hemispherical burst", ***AD-B082*, 713**.

Lee, K., Kim, T. and Kim, J. (2009), "Local response of W-shaped steel columns under blast loading", *Struct. Eng. Mech.*, **31**(1), 25-38.

Lim, C., Yao, W. and Cui, S. (2008), "Benchmark symplectic

solutions for bending of corner-supported rectangular thin plates", *IES J. Part A: Civil Struct. Eng.*, **1**(2), 106-115.
Lim, C.W., Cui, S. and Yao, W. (2007), "On new symplectic elasticity approach for exact bending solutions of rectangular thin plates with two opposite sides simply supported", *Int. J. Solid. Struct.*, **44**(16), 5396-5411.
Love, A. (2013), *A Treatise on the Mathematical Theory of Elasticity*, Cambridge University Press
Łodygowski, T., Rusinek, A., Jankowiak, T. and Sumelka, W. (2012), "Selected topics of high speed machining analysis", *Eng. Tran.*, **60**(1), 69-96.
Mannan, S. (2013), *Lees' Process Safety Essentials: Hazard Identification, Assessment and Control*, Butterworth-Heinemann.
Mazek, S.A. (2014), "Performance of sandwich structure strengthened by pyramid cover under blast effect", *Struct. Eng. Mech.*, **50**(4), 471-486.
Meleshko, V. (1997), "Bending of an elastic rectangular clamped plate: Exact versus 'engineering'solutions", *J. Elast.*, **48**(1), 1-50.
Mougeotte, C., Carlucci, P., Recchia, S. and Ji, H. (2010). "Novel approach to conducting blast load analyses using Abaqus/ Explicit-CEL", *2010 SIMULIA Customer Conference*.
Ngo, T., Mendis, P., Gupta, A. and Ramsay, J. (2007), "Blast loading and blast effects on structures–an overview", *Elec. J. Struct. Eng.*, **7**, 76-91.
Nurick, G. and Shave, G. (1996), "The deformation and tearing of thin square plates subjected to impulsive loads-an experimental study", *Int. J. Impact Eng.*, **18**(1), 99-116.
Rigby, S.E., Tyas, A., Clarke, S.D., Fay, S.D., Reay, J.J., Warren, J.A., Gant, M. and Elgy, I. (2015), "Observations from preliminary experiments on spatial and temporal pressure measurements from near-field free air explosions", *Int. J. Protect. Struct.*, **6**(2), 175-190.
Rudrapatna, N., Vaziri, R. and Olson, M. (1999), "Deformation and failure of blast-loaded square plates", *Int. J. Impact Eng.*, **22**(4), 449-467.
Shin, J., Whittaker, A.S. and Cormie, D. (2015), "TNT equivalency for overpressure and impulse for detonations of spherical charges of high explosives", *Int. J. Protect. Struct.*, **6**(3), 567-579.
Sielicki, P., Łodygowski, T., Al-Rifaie, H. and Sumelka, W. (2017), "Designing of blast resistant lightweight elevation system-numerical study", *Procedia Eng.*, **172**, 991-998.
Sielicki, P. and Stachowski, M. (2015), "Implementation of sapper-blast-module, a rapid prediction software for blast wave properties", *Central Eur. J. Energ. Mater.*, **12**(3), 473-486.
Sielicki, P.W. (2013), *Masonry Failure under Unusual Impulse Loading*, Poznan, Poland.
Sumelka, W. and Łodygowski, T. (2011), "The influence of the initial microdamage anisotropy on macrodamage mode during extremely fast thermomechanical processes", *Arch. Appl. Mech.*, **81**(12), 1973-1992.
Szymczyk, M., Sumelka, W. and Łodygowski, T. (2017), "Numerical investigation on ballistic resistance of aluminium multi-layered panels impacted by improvised projectiles", *Arch. Appl. Mech.*, DOI: 10.1007/s00419-017-1247-8.
Taylor, G. (1963), "The pressure and impulse of submarine explosion waves on plates", *Scientific papers of GI Taylor*, **3**, 287-303.
Timoshenko, S.P. and Woinowsky-Krieger, S. (1959), *Theory of Plates and Shells*, McGraw-hill
TM5-1300 (1990), *Structures to Resist the Effects of Accedental Explosions*, US Departments of Army, US Navy, Air Force, USA.
Vaziri, A. and Hutchinson, J.W. (2007), "Metal sandwich plates subject to intense air shocks", *Int. J. Solid. Struct.*, **44**(6), 2021-2035.
Wang, W., Zhang, D., Lu, F. and Liu, R. (2013), "A new SDOF method of one-way reinforced concrete slab under non-uniform blast loading", *Struct. Eng. Mech.*, **46**(5), 595-613.
Yuen, S.C.K., Nurick, G., Langdon, G. and Iyer, Y. (2016), "Deformation of thin plates subjected to impulsive load: Part III-an update 25 years on", *Int. J. Impact Eng*., **107**, 108-117
Yun, N., Shin, D., Ji, S. and Shim, C. (2014), "Experiments on blast protective systems using aluminum foam panels", *KSCE J. Civil Eng.*, **18**(7), 2153-2161.

PL